frontiers | Frontiers in Earth Science

TYPE Original Research
PUBLISHED 01 October 2024
DOI 10.3389/feart.2024.1392909

OPEN ACCESS

EDITED BY
Alex Hay-Man Ng,
Guangdong University of Technology, China

REVIEWED BY
Amir Ismail,
Texas A&M University Corpus Christi, United States
Robert Hawman,
University of Georgia, United States

*CORRESPONDENCE
Wang Shuaijun,
wsjdzj@126.com

RECEIVED 28 February 2024
ACCEPTED 18 September 2024
PUBLISHED 01 October 2024

CITATION
Song J, Wang S, Duan Y, Ye X, Lv Z, Wang L, Liu B, Song X, Cheng G and Ruan M (2024) Deep structural insights into the origin of the Heyuan ms 4.5 revealed by deep seismic sounding profiles in southeast China.
Front. Earth Sci. 12:1392909.
doi: 10.3389/feart.2024.1392909

Deep structural insights into the origin of the Heyuan ms 4.5 revealed by deep seismic sounding profiles in southeast China

Jiajia Song[1], Shuaijun Wang[1]*, Yonghong Duan[1], Xiuwei Ye[2], Zuoyong Lv[2], Liang Wang[1], Baofeng Liu[1], Xianghui Song[1], Guoliang Cheng[1] and Mingming Ruan[1]

[1]Geophysical Exploration Center, China Earthquake Administration, Zhengzhou, China, [2]Guangdong Earthquake Agency (CEA Key Laboratory of Earthquake Monitoring and Disaster Mitigation Technology, Guangdong Provincial Key Laboratory of Earthquake Early Warning and Safety Diagnosis of Major Projects), Guangzhou, China

This study presents an interpretation of a deep seismic sounding (DSS) profile that carried out along the Cathaysia Block in southeast china, aiming to explore the crustal velocity structure. Data used in the survey were obtained from three controlled-source explosions conducted along the 320 km long Lianping-Heyuan-Shanwei profile. The modeling was based on ray tracing, using the extrapolation of seismic wave arrival times with the help of travel times predicted from a one-dimensional velocity model. The average velocity structure of the middle crust is 6.0–6.4 km/s, while a low velocity anomaly of approximately 0.1–0.2 km/s in the vicinity of the Heyuan-Shaowu fault zone. The resulting 2D velocity model indicates that steeply dipping low-velocity zones that correlate with the projection of two major fault zones. These zones, together with a flat LVZ at a depth of 12 km, define a triangular region that correlates with numerous hypocenters. This tectonic setting is favorable for the accumulation and release of strain in high-velocity media within the triangular region. The unique triangular structure in the upper crust provides necessary shallow medium conditions for seismic activity. This indicates that increased seismicity within this area is partially attributed to heightened stress within higher-velocity material. The triangular annular low-velocity body, situated in the upper crust, is influenced by dynamic environmental factors caused by deep thermal disturbances. The deep-seated fault serves as a conduit for the historical migration of thermal material, likely contributing to the seismogenic conditions for earthquakes in Heyuan's region through deep-seated thermal disturbances. These findings provide a novel geophysical reference model for the regional seismicity near the Xinfengjang reservoir and significantly contribute to understanding the causal relationship between tectonic setting and seismicity. In comparison with previous studies, our research is dedicated to investigating the causes of shallow earthquakes in the region and exploring the relationship between deep and shallow structures.

KEYWORDS

southeast China, low-velocity zone, intraplate seismicity, deep-seated thermal material, the seismogenic tectonic

1 Introduction

Located in the Cathaysia Block, Heyuan exhibits persistent seismic activity, ranking among the most seismically active areas in southeast China, as indicated by seismic monitoring data. A magnitude Ms 4.5 (Epicentre at 23.84°N, 114.52°E) earthquake struck in southeast China (Figure 1C) at 5:15 a.m. on 8 March 2023. Before and after the earthquake, there were several small earthquakes. The recurrent seismic events in this area prompt inquiries regarding the correlation between the reservoir and the heightened seismicity, raising concerns about the potential onset of an active seismic period in the region. Decades of research into the seismic mechanisms in this region have consistently identified one of the prevailing influence of tectonic stress fields. This divergence underscores the complexity of the seismic nucleation process in the region (Guo and Feng, 1992). Diverse perspectives exist among researchers regarding the principal orientation of the tectonic stress. The fault structure, the stress accumulation in the structure and the underground geological conditions of the reservoir area jointly affect the seismic activity in the region (Zhang et al., 2016).

The regional tectonics in this area are notably complex, particularly in the vicinity of the Xinfengjiang Reservoir, where shallow subsurface media display conspicuous anisotropy (Shi and Gao, 2022). Presently, research efforts concerning crustal velocity structures and tectonic activities in this region primarily focus on the shallow crustal structures near the Xinfengjiang Reservoir dam area in Heyuan (Wang, 2020). To gain a deeper understanding of the seismogenic tectonic background contributing to the frequent small to moderate earthquakes in recent years, further investigation into the deep crustal structural geology of this area is crucial. Deep seismic sounding data plays a crucial role in unveiling the deep-seated structural background of seismic nucleation, providing effective insights into the velocity structure of the lithosphere and crustal structure in the study area (Moulin et al., 2023; Xiong et al., 2022; Behera et al., 2021; Zeng et al., 1988). In recent years, this approach has been widely employed to investigate the internal structure of the Earth (Liu et al., 2003; Wang et al., 2015; Deng et al., 2011; Yang et al., 2011).

Following the impoundment of the Xinfengjiang Reservoir, the stress changes induced by reservoir impoundment, in conjunction

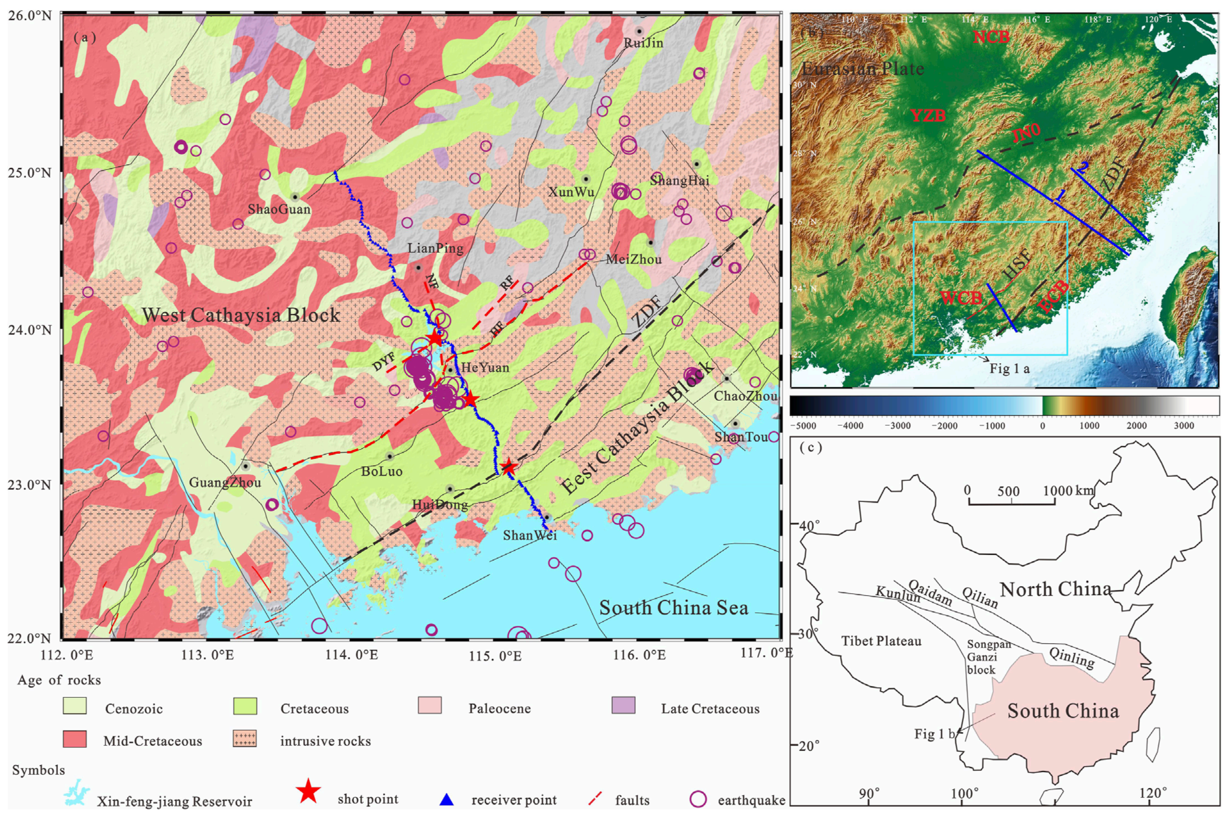

FIGURE 1
(A) Simplified geological map delineating of major structures and igneous rocks in the Yuedong and its adjacent areas. The thick dotted lines represent the main faults in Heyuan: DYF: Daping-Yanqian fault; RF: Renzishi fault; HF: Heyuan fault; NF: NNW fault. The thin black lines are major faults in mainland China. The purple circles denote Mw > 2.0 earthquakes that occurred from 2000 to 2023 downloaded from the Incorporated Research Institutions for Seismology (IRIS) website (http://ds.iris.edu/ieb/). **(B)** The location of Cathaysia Block (modified after Dong et al., 2020). The equilateral blue rectangle denotes the main research area in panel **(A)**. NCB: North China Block; WCB: West Cathaysia Block; ECB: Eest Cathaysia Block; YCB: Yangze Block; JNO: Jiang Nan Orogen. The thick dotted lines represent the main faults in Southeast China: ZDF: Zhenghe-Dapu Faults; HSF: Heyuan-Shaowu Faults. The blue lines represent the deep seismic sounding profile in Southeast China: 1. Wanzai-Hui'an deep seismic sounding profile (Lin et al., 2021); 2. Shaowu-Nanping-Pingtan deep seismic sounding profile (Li et al., 2015). **(C)** Tectonic setting of Southeast China.

with regional and tectonic stresses, collectively constitute the tectonic stress field in the area (Shen et al., 1974). During the initial stages of reservoir impoundment, the elastic load changes and pore pressure induced by reservoir seepage jointly triggered the release of regional tectonic strain energy (Zhu and Sun, 2022; Cheng et al., 2012). Over time, the impact of reservoir impoundment on seismic activity in the region has become less evident. However, certain locations remain in a critical state of rupture, where disturbances such as strengthened regional stress fields and water level changes can induce fault slip, resulting in seismic events. In summary, the intense seismic activity in the Heyuan region is attributed to the interplay of the current tectonic stress field, active faults, regional crustal structures, and reservoir impoundment. However, tectonic stress is identified as the primary driver for the accumulation and release of seismic strain energy in reservoir-induced seismicity (Zhao et al., 2016; Xu et al., 2009). Therefore, it is imperative to conduct in-depth research on the crustal structures in the region to gain a better understanding of the seismic source medium environment and dynamic processes associated with small to moderate earthquakes in the Heyuan region. However, the relationship between the deep structural system and earthquakes in this area is still unclear, which significantly hampers a comprehensive comprehension of the genesis and occurrence of small to moderate earthquakes in the Heyuan region.

The China Earthquake Administration's Geophysical Exploration Center and the Guangdong Earthquake Agency jointly completed three active-source seismic profiles in the eastern of Guangdong Province in 2021. The profile is approximately away from the epicentre of the Heyuan earthquake, with observation points spaced at an average distance of 2 km along the profile. Along the profile, 225 portable seismographs (blue triangles in Figure 1) were deployed with an average interval of about 1.2 km. The observation time was 56 days, the instrument sampling rate was 100 ms, and the main frequency was 2–10 HZ. A total of 3 controlled explosions were conducted along the seismic profile. The crustal velocity structure along the profile was obtained through three controlled-source explosions (Ye et al., 2024). Based on this, the influence of the low velocity body and the fault on the shallow earthquake and the analysis of deep structure is been redefine in this study, and the relationship between deep and shallow structure is been discussed. This study illustrates the results of the improved and consequent interpretation of deep seismic sounding profiles which provide high-resolution 2D images of the lower velocity zone (LVZ) in the crust, and that were not visible in previous studies.

2 Regional geological and tectonic setting

The Cathaysia Block is known as the spatial and temporal distribution of Mesozoic granitoid-volcanic rocks, which has occurred in changing tectonic environments in the course of geodynamic processes (Lin et al., 2021; Yan et al., 2015), and undergone several tectono-magmatic events (Shu et al., 2023; Qin et al., 2022). The study region is situated on the southeastern margin of the Cathaysia Block (Figure 1), has undergone various tectonic movements, including the subduction of the ancient Pacific Plate, expansion and closure of the ancient South China Sea, and subsequent expansion of the modern South China Sea (Li et al., 2019; Zhang et al., 2013). Numerous studies in structural geology and petrology indicate that the Cathaysia Block has undergone multiple tectonic events and magmatic processes, leading to the development of numerous dome structures and magmatic rocks in the region (Dong et al., 2020; Shu et al., 2011; Shu et al., 2015). During the Early Paleozoic, there were significant metamorphic deformation and magmatic events that impacted the middle and lower crust on a large scale (Han et al., 2023); and the Late Cretaceous, an extensional environment resulted in an intersecting system of faults accompanied by mantle magmatic upwelling (Huang et al., 2020). These tectonic events may have influenced the formation of the current tectonic pattern in the Cathaysia Block, and contributed to the complexity of the crustal structure. In the current global tectonic framework, the Cathaysia Block continues to experience westward subduction of the Philippine Plate (Li et al., 2013), with regional tectonic stress fields predominantly oriented in the NW and NWW directions (Shi and Gao, 2022). Under these influences, the primary expression of regional tectonic movements is characterised by block activities. Studies indicate that the spatial distribution of seismic activity in southeast China is influenced by the dominant block movements in the region, controlled not only by these surface movements but also by the characteristics of deep-seated crustal structures (Huang et al., 2014; Mao et al., 2014; Xu et al., 2009).

In the Heyuan region, a well-developed system of fault structures is present, characterised by the extensive distribution of three groups of discontinuous and relatively short fractures oriented in NNE, NNW, and ENE directions. These NNW, NNE, and NEE faults collectively form the Heyuan fault zone in the Cathaysia Block, and intersect a Mesozoic granitic batholith oriented in an east-west direction (Zhang et al., 2013). These faults collectively form the Heyuan-Shaowu Faults (Figure 1B). The Heyuan fault zone, which spans over a thousand kilometers in length, is cross-cutted by several active faults (Tannock and Regenauer-Lieb, 2017). This fault has an NNE and NE orientation with a southeastward dip, representing a low-angle normal fault at the crustal scale (Tannock et al., 2020). Furthermore, this fault is in a prolonged state of activity and is classified as an extensional detachment structure (Qiu et al., 2018). Adjacent to the Heyuan fault is the Renzishi Fault, which trends NNE and dips toward NW. This fault is characterised by steep inclination and strike-slip motion, with strong seismic activity in its vicinity (Wang, 2020; Liu et al., 2017). The NEE-oriented faults, such as the Nanshan-Aotou Fault, represent the main orientation of deep-seated faults (Yang et al., 2013), is considered a deep-seated main structural element within this fault group. Fault structures with steep dip angles, combining strike-slip and normal faulting, are prone to instability (Ye et al., 2017). This region falls within a crustal extensional tectonic zone, it exhibits a crustal-scale decoupling with characteristics of ductile strike-slip shear zones in the present day (Li et al., 2020). In the vertical direction, multiple NNE-oriented fault endpoints and intersections with faults of other orientations are observed in the area from the dam of the Xinfengjiang Reservoir to the canyon region (Yue et al., 2008).

3 Data processing methods

Considering the narrow-band characteristics of the portable seismographs, it is necessary to de-instrument the data to enhance the amplitude of low-frequency signals. We preprocessed the intercepted data, including deburring, de-average, de-line trend and waveform pinch-out, resampling. Then the P-wave data was filtered in the frequency range of 2–10 Hz. The travel times of all phases were picked by ZPlot, which is a interactive plotting and picking software package (Zelt and Smith, 1992). The combination of phase comparison and waveform correlation was utilized to identify the seismic phases within the waveform groups obtained along the profile. Seismic rays along the profile are not strictly two dimensionally distributed, so we use orthogonal projection to move the source and receiver points to a straight line. The travel data were processed with T^2-X^2 method and the VELEST inversion approach to determine a 1-D crustal velocity model (Wang et al., 2015; Kissling et al., 1995). Then, we use the 2D finite-difference inversion method (Guo and Feng, 1992; Vidale, 1990) to get the upper crustal velocity model (Figure 7B). Based on this, the initial 2D crustal structure was builded. The final 2D velocity crustal structure were obtained through two-dimensional ray tracing and trial and error modelling techniques (Song et al., 2024).

3.1 Seismic phase identification and comparison

The seismic phases were identified and compared by using an equivalent velocity of 6.0 km/s (Figure 2). Several seismic phases were recorded, including the refracted phases in the upper crust (Pg), crustal reflected phases (P1, P2, P3), refracted phases from the Moho interface (Pm), and refracted phases in the uppermost mantle (Pn). Pg and Pm are the dominant phases, with strong energy. The Pg arrivals may be traced at offset up to 130 km, while the Pm is apparent at 50–180 km. P1, P2 and P3 are relatively continuous, and it display relatively strong amplitudes in certain sections. Pn with weak amplitude shows clear onset and may be traced around 160 km.

3.2 The crust-mantle velocity structure model

Due to limited coverage of the obeservations on the profile, it is crucial build ray tracing modeling with additional constraints from earlier seismic studies (Tiira et al., 2022). This model, combined with regional a priori stratigraphic information and seismic phase analysis, facilitates the determination of the interface between inner crustal layers (Li et al., 2019; Ye et al., 2020; Lin et al., 2021). Using the Seis series package (Cerveny and Hron, 1980; Červený and Pšenčík, 1984; Cerveny, 2001), which is commonly used to process travel time data, the forward fitting method is used to carry out dynamic ray tracing and travel time fitting in two-dimensional in-homogeneous media for the P-wave travel time data set obtained. Under the constraint of the seismic phase information, the model is adjusted repeatedly to calculate the theoretical travel time and the synthetic seismic map, so as to achieve the best fit between the calculated time and the picked time (Figure 3). On the basis of the above work, the final 2D velocity model along the profile are obtained.

Previous study have founding that when using forward ray-tracing to model of deep seismic sounding data, the final result is very dependent on the interpreter's knowledge of the area and experience (Cerveny, 2001; Majdanski and Polkowski, 2014). In order to analyze the accuracy of the final model, we take the Pm phase ray tracing of Sp1 as an example. Based on the obtained optimal two-dimensional velocity model, the ray tracing operations of D ± 0.2 km, D ± 0.6 km, V ± 0.05 km/s and V ± 0.15 km/s are performed respectively (Figure 4). Compared with the final model, it is found that when the speed changes ±0.05 km/s and the depth changes ±0.2 km, the calculated time deviates from the picked time. The result prove that the final the 2D P-wave velocity model is close to the actual situation in the region.

To further obtain the quantification of 2D model uncertainty evaluation results, we choose the multi-parameter uncertainty evaluation method (Majdanski, 2013). This method used a simplified ray propagation in 1D layered media and the error propagation theory, which assigns the uncertainty of the model depth and velocity to the travel times. Based on the simplified 2D gridded velocity model (1 km × 0.1 km), the model is transformed into multiple one-dimensional velocity models with four interfaces (G, C1, C2, M). Based on the assumption of constant velocity in each layer, the boundary depth errors and crust velocity errors were estimated for each 1D model (Song et al., 2024; Majdanski and Polkowski, 2014). The uncertainty results of each 1D model were systematically combined to form the final uncertainty results of the 2D model (Figure 5). The estimated results show that the average velocity uncertainty of each crustal layer is ±0.028 km/s, ±0.034 km/s, ±0.14 km/s, ±0.32 km/s and ±0.45 km/s, and the average uncertainties of different interfaces depth are ±0.32 km, ±0.6 km, ±1.4 km and ±2.1 km, respectively.

4 The results

4.1 Characteristics of upper crustal media

On the seismic phase, the phases P1 and P3 can be read, and the far ends of these two sets of seismic phases are parallel to the far end of the Pg wave. For a uniform positive gradient, the slope (velocity) of the P1 phase will be greater than that of the Pg phase, and the tail ends of the two sets of seismic phases are parallel (Figure 2). It is speculated that there is a low-velocity body or a low-velocity layer between the P1 layer and the Pg layer. If the LVZ does not exist, the tails of Pg and P1 will intersect according to the normal formation velocity gradient. Similarly, there are also low-velocity bodies or low-velocity layers between the P1 layer and the P3 layer. So we did an experiment, when these anomalies are removed from the 2-D velocity model, the deviation between the theoretical travel time and the measured travel time will be large (Figure 4F). Therefore, this study focuses on the two different depth ranges (0–5 km and 0–20 km) respectively, with the 2D grid being equalised to highlight the effective information (Figures 6).

The velocity structure near the Heyuan region (Figure 6B) reveals significant lateral heterogeneity in the upper crustal media,

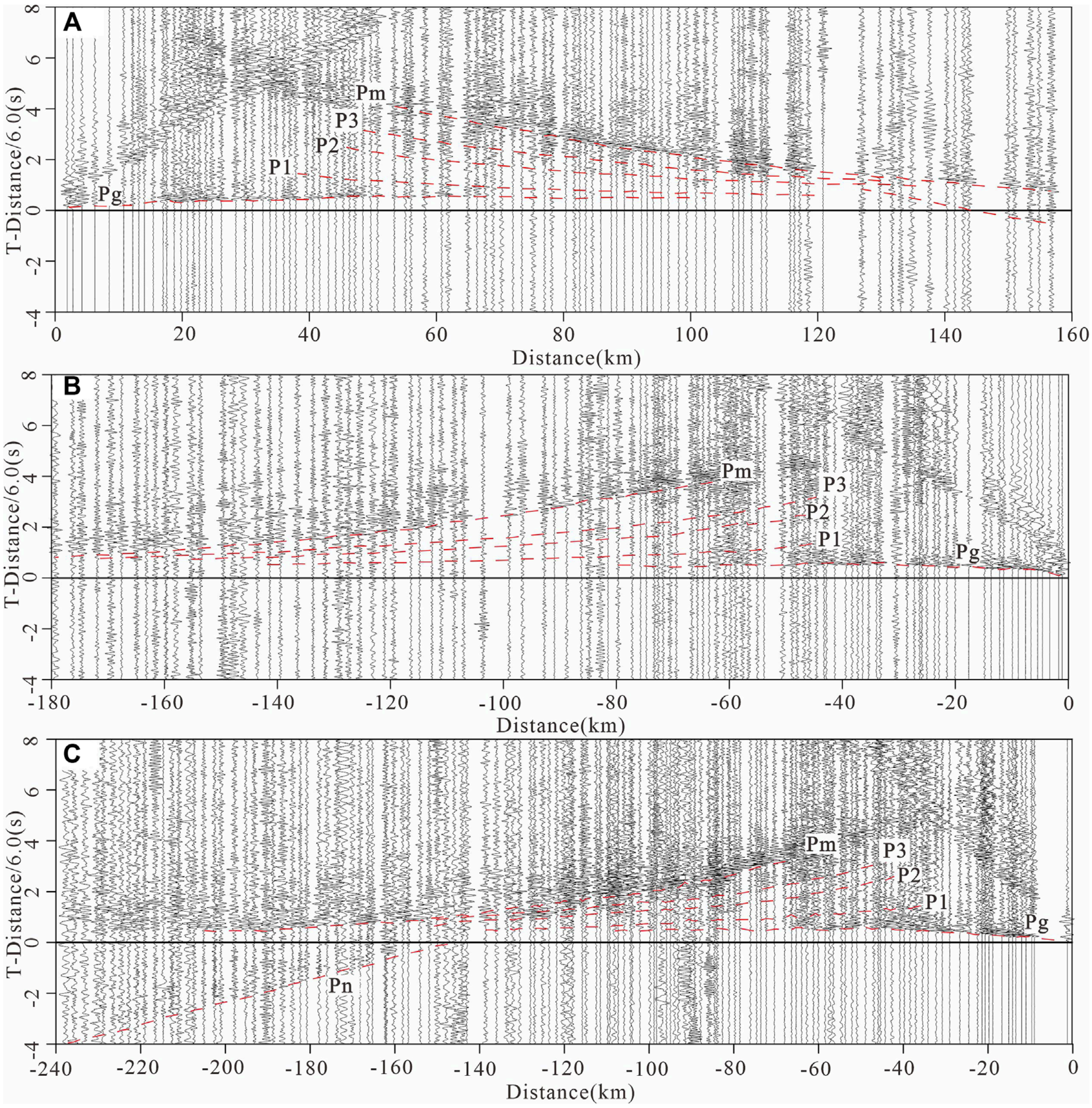

FIGURE 2
Typical seismic record sections in the Heyuan-Lianping-Shanwu profile (reduced velocity of 6.0 km/s). **(A)** Shotpoint Sp1, right branch observation. **(B)** Shotpoint Sp2, left branch observation. **(C)** Shotppoint Sp3, left branch observation.

with an undulating basement surface. This basement structure implies multiple modifications to the crystalline basement in the region since the Cenozoic era (Tian et al., 2020; Jia et al., 2009). A LVZ with a velocity of 5.90 km/s appears in the upper crust, the depth of it approximately is 12 km (Figure 6). The corresponding lower boundary of the upper crustal structure shows a slight uplift. The Ms 4.5 Heyuan earthquake occurred at the edge of the LVZ1, same as the historical earthquakes at the position where the velocity gradient changes in the upper part of the LVZ.In the upper crust of this area, two distinct types of LVZs are identified. Among which, LVZ1 is a nearly horizontally oriented LVZ at the base of the upper crust. The LVZ1 is closely related to geological structures, fault zones, and stress environments (Zhou et al., 2020; Cheng et al., 2012). The second type is the fault zone, which extends from the surface towards deeper layers, constituting the LVZ2. These two LVZs spatially configure a triangular ring of low-velocity material on three sides, while the central area is relatively composed of high-velocity material compared to the surrounding three sides. The LVZ2 correspond to the NW-dipping Daping-Yanqian and Renzishi faults and the SE-dipping Heyuan fault, respectively. Considering the material fragmentation within the fault zones, the relatively lower P-wave velocities observed from the surface to the shallow upper crust can be interpreted as the fault-fractured zone exhibiting an inverted "V" shape. The fractured fault system facilitates the infiltration of reservoir water, and under the influence of water pressure and infiltration, the permeation along the fault channels leads to localised uneven fluid pressure increases (Guo et al., 2022; Dong et al., 2022). This alteration in the behaviour of regional fault sliding has, to some extent, induced regional strain instability.

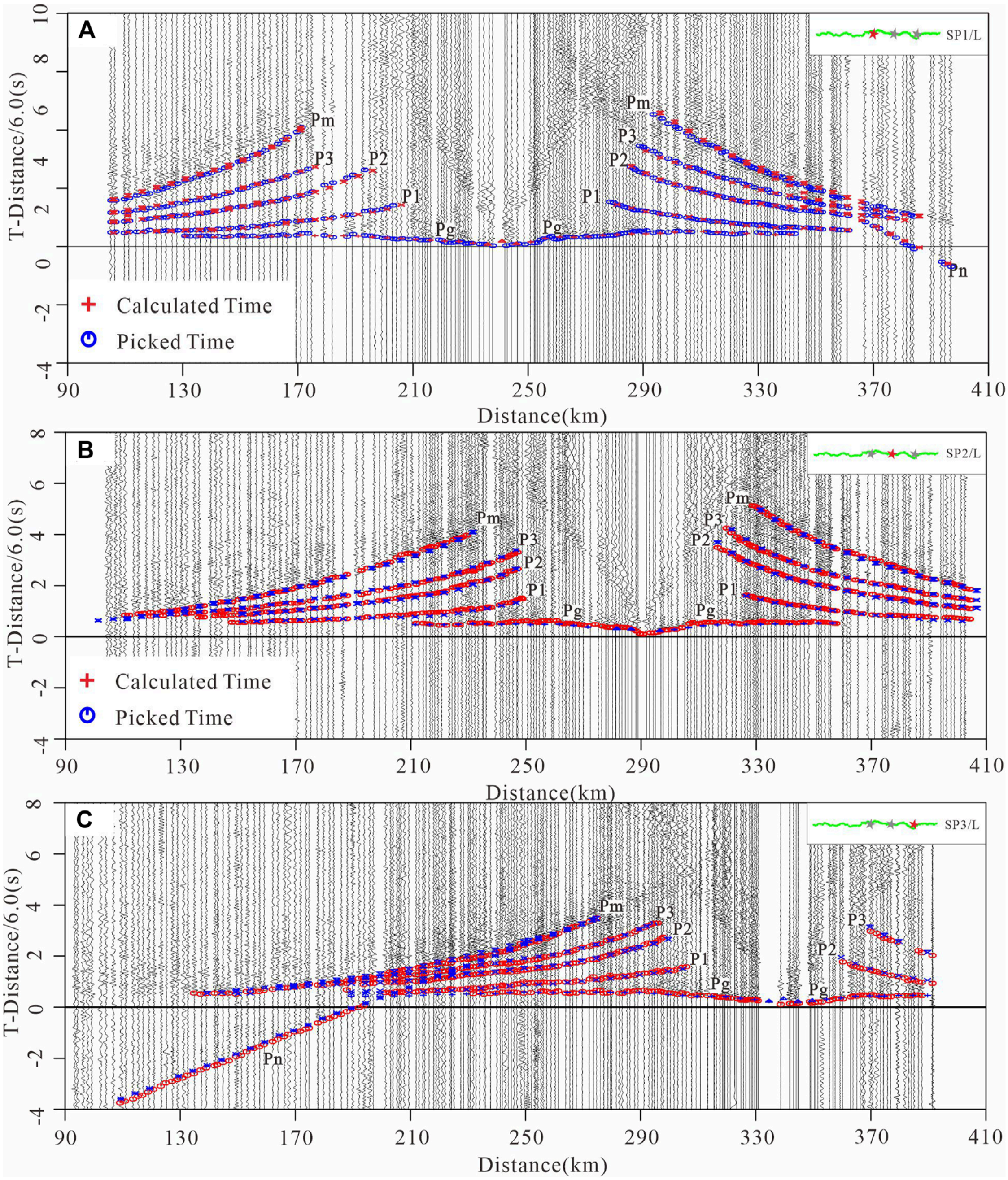

FIGURE 3
Theoretical and observed seismic waveforms with a reduction velocity of 6.0 km/s; red crosses and blue circles indicate picked times and calculated times. **(A)** Shotpoint Sp1. **(B)** Shotpoint Sp2. **(C)** Shotpoint Sp3.

The differential physical properties of the brittle upper crust rocks and formations play a crucial role as essential medium conditions for the incubation and occurrence of earthquakes (Zhang et al., 1994; Jia et al., 2006; Xu et al., 2017; Xia et al., 2021). This unique annular triangular-shaped LVZ in the upper crustal may contribute to the favourable conditions for the occurrence of small to medium-sized earthquakes in the Heyuan region. In the high-low-velocity transition zone of the rock, where the strength is relatively higher, stress accumulates more easily. The adjacent relatively high-velocity region to the LVZ provides the conditions for brittle deformation in the upper crust, while the LVZ facilitates the accumulation of regional strain energy, acting as a stress transfer medium. As a zone of mechanical weakness in the crust, the LVZ plays a role as a lower boundary and decoupling zone during the movement and interaction of blocks (Yang et al., 2003; Wan et al., 2022). Under the same tectonic stress field, the upper crustal block on the side with the LVZ is more prone to slipping, furthermore, it may serve as a regulator for regional

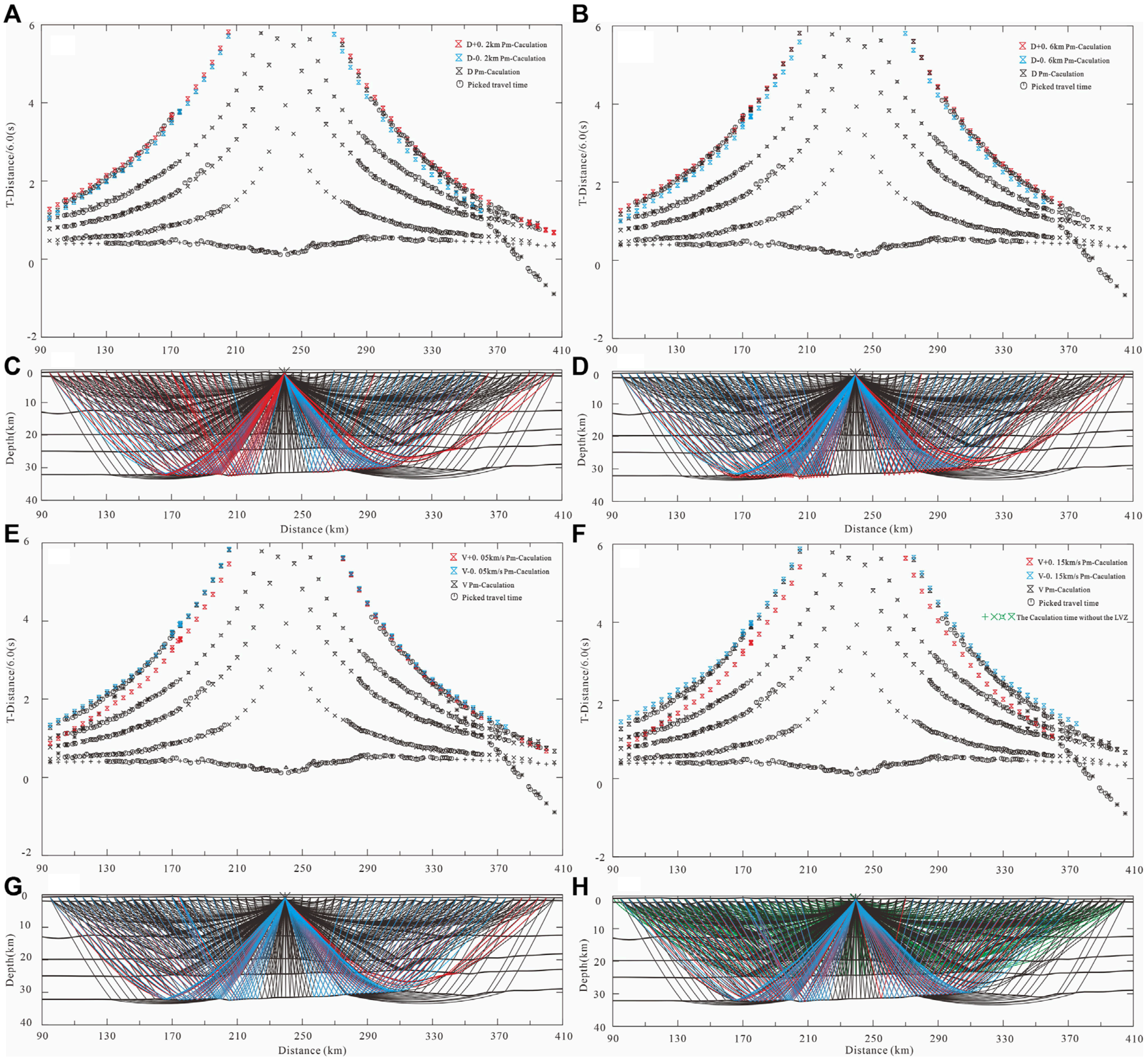

FIGURE 4
(A, B, E, F) Fitting between observed and synthetic P-wave travel times obtained by forward computation using the ray tracing method, with reference to the shot point Sp1 and the Lianping-Heyuan profile; **(C, D, G, H)** Ray diagram showing the illumination of the crust by ray coverage along the profile. Error analysis of the Sp1 for ray tracing. **(A)** D ± 0.2 km. **(B)** D ± 0.6 km. **(E)** V ± 0.05 km/s **(F)** V±0.15 km/s; The green symbol represents calculation time with these anomalies (LVZ) are removed from the 2-D velocity model.

stress balance in the process of regional strain energy accumulation (Cao et al., 2014). However, .the true geological condition cannot be determined from a 2D section and out-of-plane reflections can lead to misinterpretations of in-plane features (Westgate et al., 2022). The subsequent detailed analysis of the shallow seismic structure in this area needs more favorable three-dimensional geophysical data to demonstrate.

4.2 Deep structural configuration

The C1 interface, the C2 interface and the Moho interface occur at depths of 15 km, 25 km, and 31 km (Figure 7), respectively, which is close to the results of previous studies (Figure 8)on the crustal structure of the Cathaysia Block (Lin et al., 2021; Li et al., 2015; Li et al., 2013). The Moho is at a depth of 30.0 km in the East Cathaysia Block, and that gradually deepens to the Weat Cathaysia Block to 32.0 km at position 220 km along the profile. From the East Cathaysia Block to the West Cathaysia Block, there is an apparent uplift of the C3 and Moho interfaces, accompanied by pronounced ductile deformation in the lower crust (Figure 8). Notably, the extent of extensional deformation in the ductile lower crust is greater than that in the brittle upper crust. This phenomenon may be correlated with deep-seated magmatic activity in the Cathaysia Block. Considering the rich geothermal resources distributed along the Heyuan fault zone in this region, it is speculated that there might be deep-seated thermal material flow.The interaction between the mantle and the

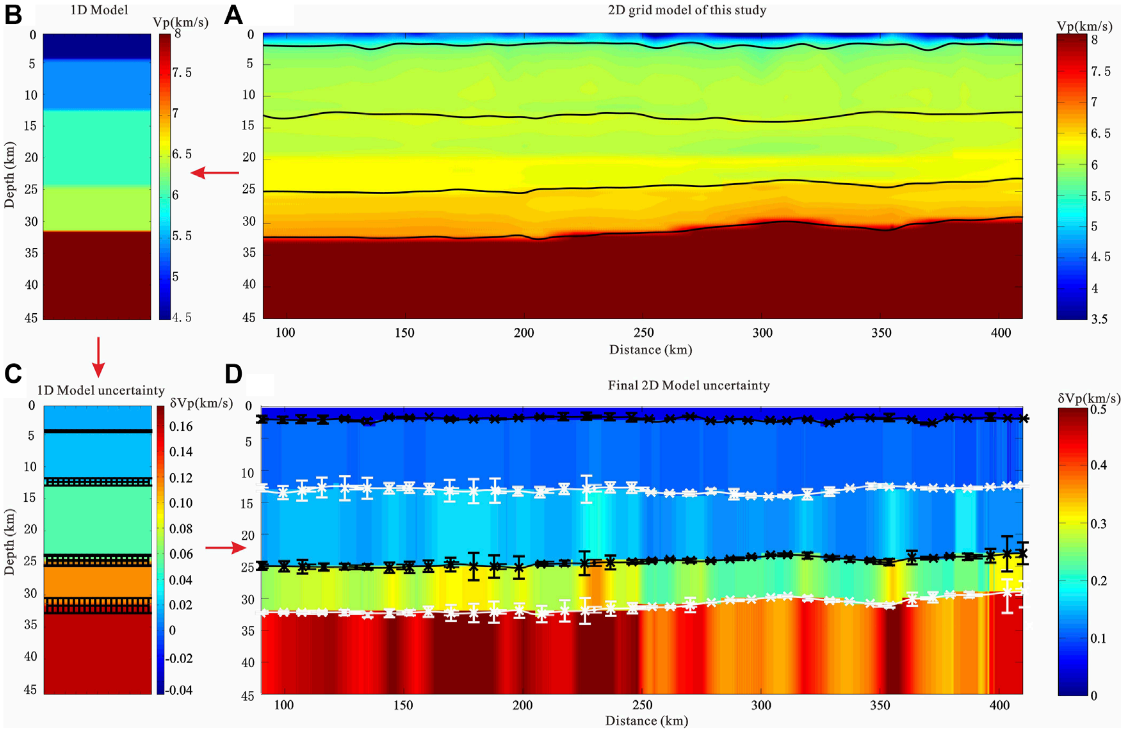

FIGURE 5
Flow chart of uncertainty evaluation with multi-parameter method (Majdanski, 2013). **(A)** Simplified 2D grid velocity model in this study. **(B)** 1D model extracted from the 2D model with 1 km interval. **(C)** The uncertainty estimation is depicted using the simplified 1D model, with color bars indicating the uncertainty of velocity and error bars representing the uncertainties of boundary depth. **(D)** The uncertainty evaluation result of 2D velocity model. Colors bars mark the uncertainty of velocity and error bars mark the uncertainties of boundary depth.

crust, facilitated by magmatic processes, may compensate for the thinning effect on the lithosphere caused by extensional tectonics (Dong et al., 2023; Zhou et al., 2020). This process results in a relatively gentle and flat Moho interface. The upwelling material has also contributed to the modification of the lower crust, promoting crustal extensional thinning and enhancing the fluidity of the lower crust (Dong et al., 2020). In the region beneath the Heyuan fault zone, delineated by the fault itself, a discernible lateral variation in velocity structure is observed from the basement to the Moho interface. Proximal to the Heyuan fault zone, significant lateral velocity structure discrepancies are evident in the mid-to-upper crust. Moreover, this lateral heterogeneity extends consistently toward the vicinity of the Moho interface, providing robust deep-seated data support for the incision of deep-seated faults through the middle crust in this region. Along this deep-seated structural zone, geothermal resources are abundant, and the convergence zones of faults serve as major conduits for the ascent of thermal springs (Nazeri et al., 2023). Field exposures reveal multiple episodes of activity along the footwall of the Heyuan fault, characterised by fractured silicified zones and the intrusion of multiple generations of quartz veins (Tannock et al., 2019). Considering the presence of a soft asthenospheric uplift beneath the deep fault zone, it is inferred that the Heyuan fault zone, similar to other NE-trending deep-seated fault zones within Guangdong Province, serves as a pathway for the upward migration of deep-seated thermal material (Cao et al., 2022; Li, 2021).

5 Discussion

The P-wave velocity in the fracture zone is usually lower than that in the surrounding rock, while the mean velocity below the river source is obviously lower (Figure 9). Due to the development of surface hot springs in this region, and the predecessors pointed out that the low crustal average velocity corresponds to the development of high-temperature magma (Wang et al., 2015), and deep and large faults developed here, suggesting that there was multiple fracturing and fluid flow events occurred. Given that the deep seismic sounding profile is two-dimensional, it is imperative to ensure the presence of low velocity bodies beneath the earthquake's location in Heyuan region. To accomplish this, we utilize results from previous studies for velocity slice analysis (Yang et al., 2021). It can be seen that in the two horizontal slices shown in Figure 10, the Heyuan area exists at the juncture of high and low velocities. Furthermore, there are low velocity bodies situated south of the middle upper crust river source area, which may be related to magmatic-hydrothermal activity. The Cathaysia Block has undergone multiple episodes of mantle thermal activity, with deep-seated faults providing conduits for the flow of deep-seated thermal material (Lin et al., 2023; Xia et al., 2021; Xie et al., 2001). Approaching the phenomenon from various geophysical perspectives, scholars have presented evidence for deep-seated thermal material flow in this region (Huang et al., 2014; Xi, 2021; Wang et al., 2022). Deep-seated thermal material migration towards

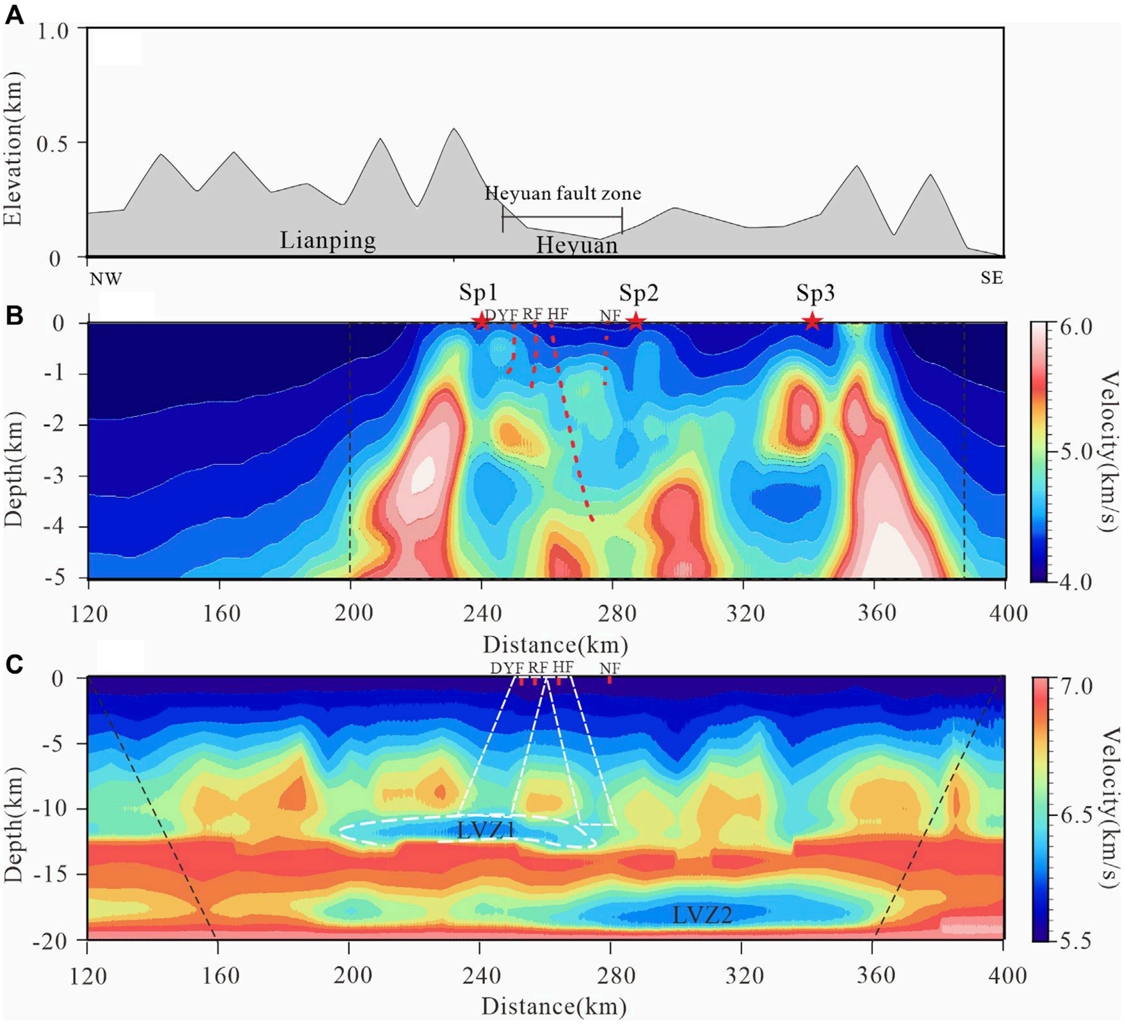

FIGURE 6
Velocity structure diagram of middle and upper crust in Heyuan and its adjacent area (The resolution between the black dashed line and the border is lower than in other areas.). **(A)** Terrain profiles. **(B)** The velocity section of 0–5 km. **(C)** The velocity section of 0–20 km.

the lower crust generates upward-directed vertical tectonic stress (Zeng et al., 1985). A certain correlation exists between the vertical tectonic stress and the seismic location (Zhang et al., 2022; She et al., 2017). Hence, the upwelling of thermal material inducing vertical tectonic stress might provide the deep-seated dynamic environment for the occurrence of small to moderate shallow earthquakes in the Heyuan region. In the meantime, the two lower LVZs may play a role in facilitate upward migration of magma.

The structural relationship between secondary shallow faults and regional deep-seated faults plays a crucial role in determining the seismic hazard potential of the region. The upward vertical tectonic stress generated by the upwelling of deep-seated thermal material is a significant characteristic of the middle crust, marked by two horizontally oriented LVZs at depths of 20 and 25 km (Figure 10). These LVZs often coincide with weakened geological layers in the region, allowing for the control of present-day intra-plate deformation and seismic activity by adjusting the local-scale strain distribution (Zhou et al., 2020; Tarayoun et al., 2019). The LVZs developed in the middle crust, however, play a role in concentrating strain. The middle crust is prone to diffuse creep deformation (Willis et al., 2019), displaying characteristics of brittle-ductile transition zones. The middle crust does not accumulate strain energy but concentrates the vertical tectonic stress generated by the upwelling of deep-seated heat sources (Zeng et al., 1985). This concentrates necessary energy for seismic events, potentially promoting the localisation of strain in adjacent shallow-seated seismogenic structures (Zuza et al., 2022). Consequently, strain energy accumulates rapidly and is released in the brittle upper crust (Sibson, 1983). In summary, the shallow crust provides the environmental conditions for seismogenic structures, while the deep structures offer the dynamic background for seismic nucleation.

Localized thinning of the crust derived from the wide-angle data correlates with previous imaging of low-Vs anomalies in the middle to lower crust (Figure 10), suggesting a possible conduit for the upward migration of hot material, contributing to stress

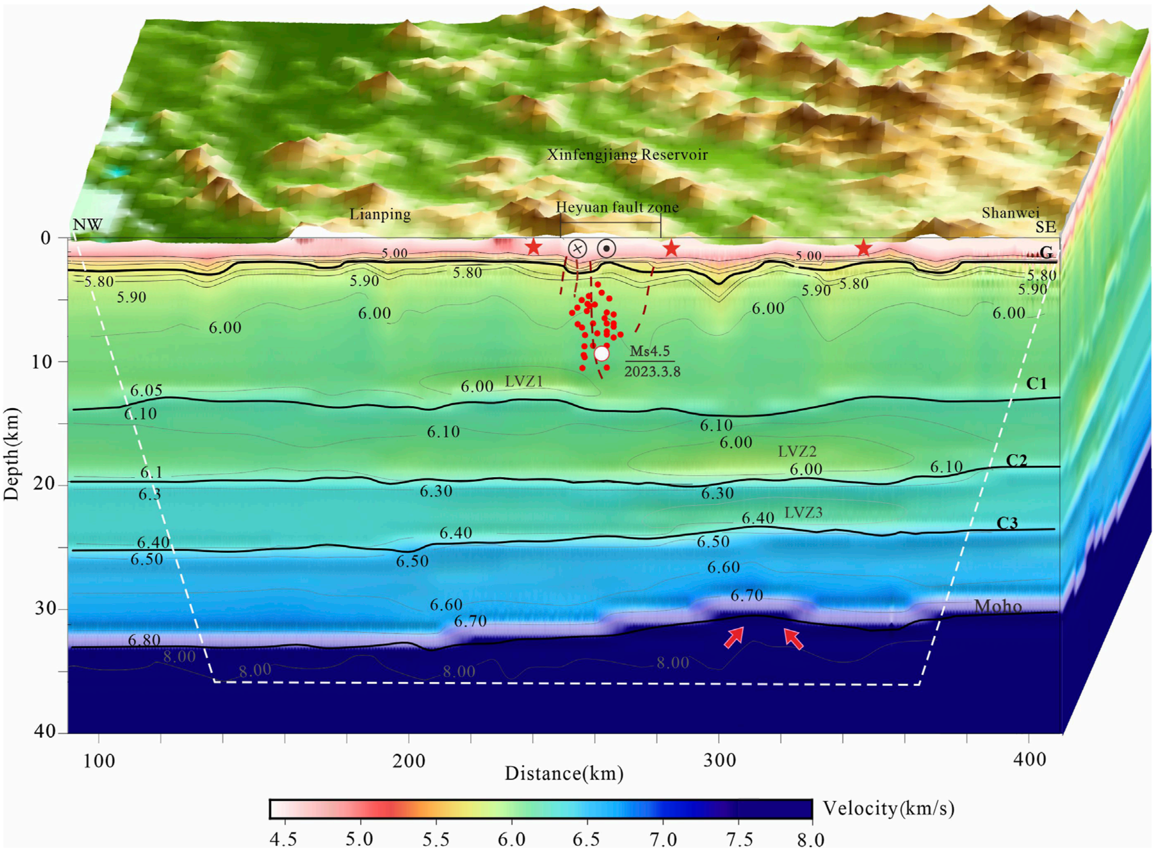

FIGURE 7
Crust structure velocity of Heyuan area. The red dot are Mw > 2.0 earthquakes that occurred from 2000 to 2023 in this region, which downloaded from the Incorporated Research Institutions for Seismology (IRIS) website (http://ds.iris.edu/ieb/).

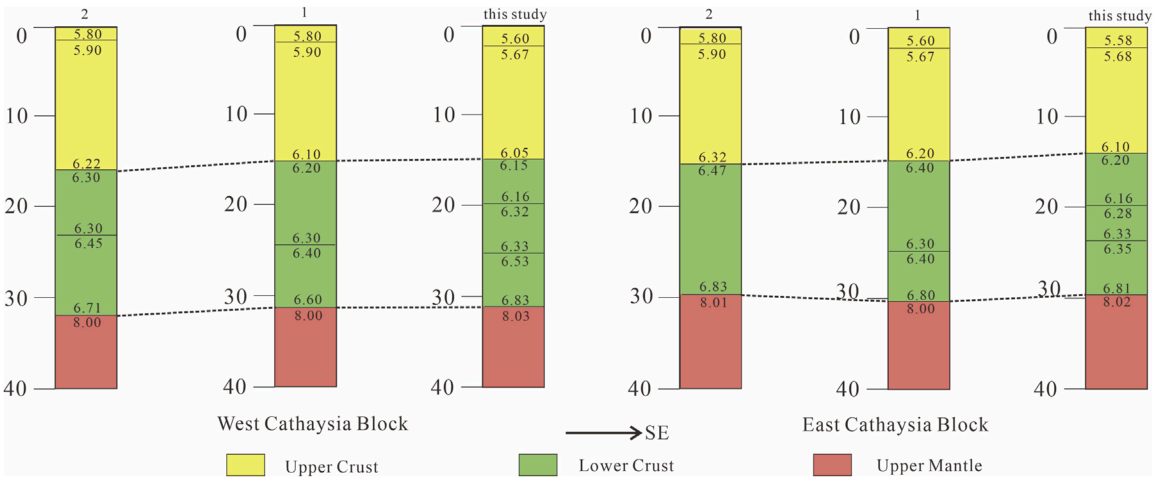

FIGURE 8
Comparison of the results of the present and previous studies in Cathaysia Block. 1. Wanzai-Hui'an deep seismic sounding profile (Lin et al., 2021); 2. Shaowu-Nanping-Pingtan deep seismic sounding profile (Li et al., 2015).

closer to the surface, and the region's geothermal resources provide direct evidence of heat sources at depth. The relatively strong crust enables the elevated stresses within the triangular zone reactivating pre-existing faults with it and subsequently triggering earthquakes. A similar mechanism has been documented in other intraplate seismicity areas such as the Flinders Ranges in SE Australia

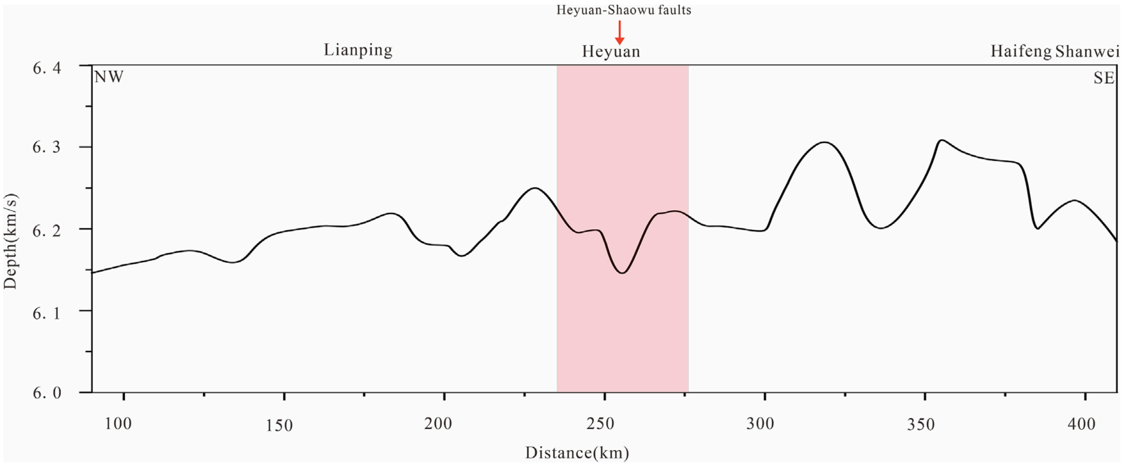

FIGURE 9
Average crustal velocity structure of the Lianping-Heyuan-Shantou profile.

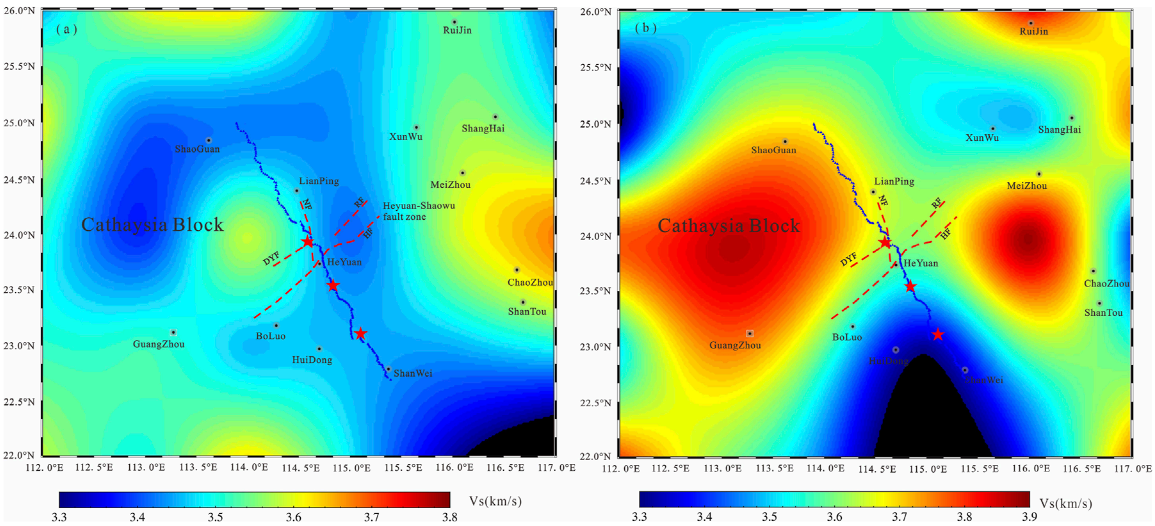

FIGURE 10
Vs. velocity slice from Multi-Observable Probabilistic Inversion study (Yang et al., 2021). **(A)** 14 km, **(B)** 24 km. The red pentagrams are shot-point, the blue triangles are receiver, and the red lines are faults.

(Balfour et al., 2015). The deep fluids may serve as conduits that gather and channel these fluids from the mantle and the lower crust into the brittle crust, where they increase pore-fluid pressure and trigger seismic events (Nyamwandha et al., 2016). Whether the intraplate seismicity are triggered by tectonic loading or by local stress perturbation remians an open question (Craig et al., 2017). This mechanism may not documented in other intraplate areas, require local tectonic strsssess or strain accumulation to interpret intraplate seismicity. The controlling factor appears to be a localized thinning of the lithosphere that focuses stress within the brittle part of the subsurface in the New Madrid fault zone (Leclère and Calais, 2019; Zhan et al., 2016). Elsewhere in the central U.S., some intraplate seismicity has been associated with steep gradients in gravity inferred to mark the edges of mafic intrusions (Braile et al., 1982; Hildebrand and Easton, 1995). It can be seen that researchers have different definition of the genetic mechanism of intraplate shallow seismicity in different plates. On the one hand, it is the lack of direct understanding of the source medium environment and dynamic process in geophysical exploration. On the other hand, it is the complex diversity of the tectonic causes of different plates.

6 Conclusion

This study utilizes the velocity structure model obtained from controlled-source seismic depth sounding to provide insights into the deep structural characteristics of the Heyuan region.

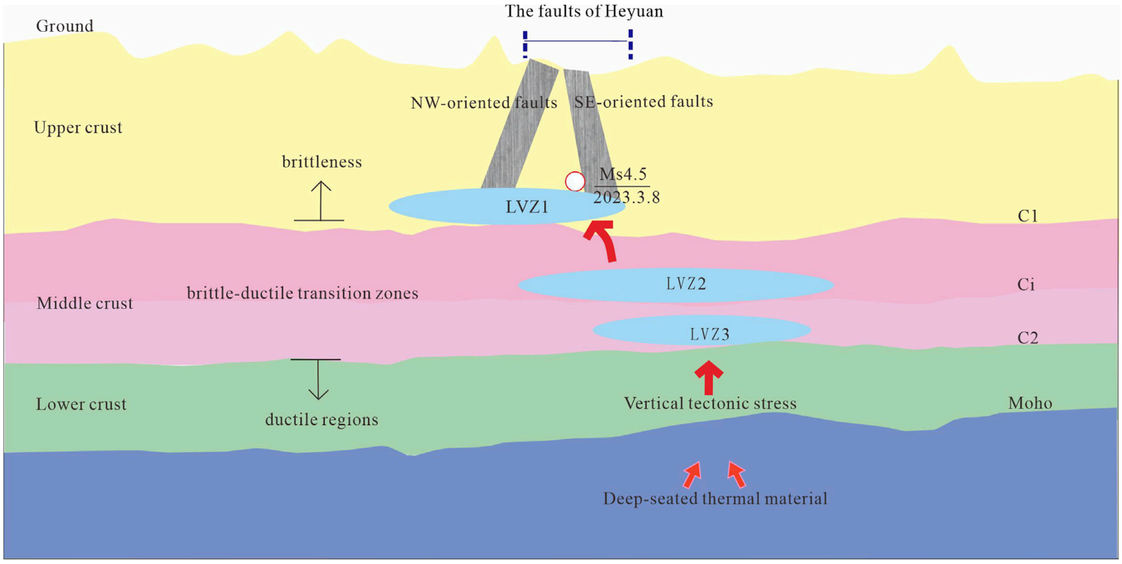

FIGURE 11
Simplified structural map of small and medium earthquake generation and inception in Heyuan area.

6.1 Medium properties of the hypocentre area

The region exhibiting the most significant variation in crustal velocity along the profile is situated to the north of the Heyuan region. Within the lower part of the upper crust, at a depth ranging from 10–12 km, there exists a horizontally-oriented LVZ. This LVZ, in conjunction with a fractured fault zone, collectively forms an annular triangular-shaped LVZ. Previous research has indicated that earthquakes of moderate intensity often occur in regions where there is a transition between low- and high-velocity zones, with a tendency to favor the side of the high-velocity body (Liu et al., 2003). Therefore, it can be inferred that lateral variation in the physical properties of the upper crust within our study area provides conducive medium conditions for occurrences such as the Heyuan Ms 4.5 earthquake and other small to moderate seismic events within this region. Future studies could focus on areas of strain instability within regional upper crusts and include integrated detection and evaluation of seismic environments through various geophysical means. At the same time, quantitative source parameter calculation should be carried out in future related research (Nazeri et al., 2023).

6.2 Dynamical background of the hypocentre area

The Heyuan Fault region is rich in geothermal resources, as indicated by geochemical analyses showing the presence of intermediate-acidic syntectonic rock veins at various intervals within the extensional detachment zone (Tannock et al., 2020). It is hypothesized that the ductile shear zone actively contributes to the deformation process, creating deep thermal disturbance dynamics conducive to minor earthquakes in this area. The decoupling effect between deep and shallow faults establishes a profound tectonic context for the nucleation and initiation of earthquakes. The deep thermal disturbances induce direct or indirect alterations in local strain rates, placing the brittle upper crust in a state of critical strain instability highly susceptible to triggering and forming earthquakes. Building on previous analysis (Zeng et al., 1985), it is inferred that deep-seated thermal disturbances contribute to stress energy accumulation, providing dynamic force for seismic events.

6.3 Seismogenic structure and tectonics

The region's frequent seismic activity is intricately linked to the pronounced heterogeneity of its regional media and the multifaceted context of seismic structural construction. The region's unique crustal structural feature, the annular triangular low-velocity body, combined with the decoupling effect between deep and shallow faults, forms the triggering structure for these frequent seismic events (Figure 11). These junctions between faults are prone to experiencing concentrated regional stress and strain distribution. The decoupling effect between deep and shallow faults establishes the structural background for seismic genesis and release. Faults converging in the upper crust, where strain energy is prone to accumulate, may lead to localized stress concentration, triggering a state of strain instability and giving rise to small to moderate earthquakes. The reservoir acts as a triggering factor for these seismic events. In the reservoir area and its surroundings, hydraulic permeation increases pore pressure, thereby weakening rock strength (Mackwell et al., 1998). This process intensifies the occurrence of small to moderate earthquakes in the region by unfavourably affecting regional strain energy accumulation. In future work, further studies are needed that pay more attention to understanding deep tectonic backgrounds before constructing a reservoir. However, only using two-dimensional exploration data to reflect three-dimensional underground media is one-sided. The subsequent detailed analysis of the shallow seismic structure in this area needs more favorable three-dimensional geophysical data to demonstrate in the future.

Data availability statement

The data analyzed in this study is subject to the following licenses/restrictions: research work. Requests to access these datasets should be directed to Shuaijun Wang, wsjdzj@126.com.

Author contributions

JS: Writing–original draft. SW: Writing–original draft. YD: Writing–original draft. XY: Writing–review and editing. ZL: Writing–review and editing. LW: Writing–review and editing. BL: Writing–review and editing. XS: Writing–review and editing. GC: Writing–review and editing. MR: Writing–review and editing.

Funding

The author(s) declare that financial support was received for the research, authorship, and/or publication of this article. This study was supported by the National Natural Science Foundation of China (No. 41474076), Geophysical Exploration Center Youth Fund (No. YFGEC2022003), Open Research Fund of the Key Laboratory of the Ministry of Education "Tectonics and Hydrocarbon Resources" (No. TPR-2022–03).

Acknowledgments

We are grateful to thank Prof.Fuyun Wang for the guidance during the writing of this paper. We thank the editor and two reviewers for their constructive comments.

Conflict of interest

The authors declare that the research was conducted in the absence of any commercial or financial relationships that could be construed as a potential conflict of interest.

Publisher's note

All claims expressed in this article are solely those of the authors and do not necessarily represent those of their affiliated organizations, or those of the publisher, the editors and the reviewers. Any product that may be evaluated in this article, or claim that may be made by its manufacturer, is not guaranteed or endorsed by the publisher.

References

Balfour, N. J. P. R. C., Pilia, P. R., and Love, D. (2015). Localization of intraplate deformation through fluid-assisted faulting in the lower-crust: the Flinders Ranges, South Australia. *Tectonophysics* 655, 97–106. doi:10.1016/j.tecto.2015.05.014

Behera, L., Kolluru, R., and Singh, B. (2021). Imaging Mesozoic sediments in Deccan Volcanic province of India: inferences from seismic and gravity studies. *J. Geol. Soc. India* 97, 1260–1273. doi:10.1007/s12594-021-1855-3

Braile, L. W., Keller, G. R., Hinze, W. J., and Lidiak, E. G. (1982). An ancient rift complex and its relation to contemporary seismicity in the new Madrid seismic zone. *Tectonics* 1 (2), 225–237. doi:10.1029/TC001i002p00225

Cao, J. H., Sun, J. L., Xu, H. L., and Xi, S. H. (2014). Seismological features of the littoral fault zone in the Pearl River Estuary. *Chin. J. Geophys. (in Chinese)* 57 (2), 498–508. doi:10.6038/cjg20140215

Cao, L., Yuan, H., Zhao, L., Zhao, M., Huang, H., Hao, T., et al. (2022). Fault-controlled regional magmatism and mineral deposition in central Cathaysia-Evidence from ambient noise tomography. *Science China Earth Sciences* 65 (9), 1715–1735. doi:10.1007/s11430-021-9941-2

Cerveny, V. (2001), 110. Cambridge: Cambridge University Press. doi:10.1115/1.1508173

Cerveny, V., and Hron, F. (1980). The ray series method and dynamic ray tracing system for three-dimensional inhomogeneous media. *Bull. Seismol. Soc. Am.* 70 (1), 47–77.

Červený, V., and Pšenčík, I. (1984). Gaussian beams in elastic 2-D laterally varying layered structures. *Geophysical Journal International* 78 (1), 65–91. doi:10.1111/j.1365-246X.1984.tb06472.x

Cheng, H. H., Zhang, H., Zhu, B. J., Sun, Y. J., Liang, Z., Yang, S. H., et al. (2012). Finite element investigation of the poroelastic effect on the Xinfengjiang Reservoir-triggered earthquake. *China ScienceEarth Science* 42 (06), 1942–1952. doi:10.1007/s11430-012-4470-8

Craig, T. J., Chanard, K., and Calais, E. (2017). Hydrologically-driven crustal stresses and seismicity in the new Madrid seismic zone. *Nature communications* 8 (1), 2143. doi:10.1038/s41467-017-01696-w

Deng, Y. F., Li, S. L., Fan, W. M., and Liu, J. (2011). Crustal structure beneath South China revealed by deep seismic soundings and its dynamics implications. *Chinese Journal of Geophysics (in Chinese)* 54 (10), 2560–2574. doi:10.3969/j.issn.0001-5733.2011.10.013

Dong, P., Ran, X., Yang, H. F., Guo, Z., and Xia, K. (2022). Fault slip behaviors modulated by locally increased fluid pressure: earthquake nucleation and slow slip events. *Journal of Geophysical Research Solid Earth* 127 (12), e2022JB024612. doi:10.1029/2022JB024612

Dong, S., Li, J., Gao, R., Cawood, P. A., Thybo, H., Johnston, S. T., et al. (2023). Intraplate lithospheric extension revealed by seismic reflection profiling of South China. *Earth and Planetary Science Letters* 609, 118100. doi:10.1016/j.epsl.2023.118100

Dong, S. W., Li, J. H., Cawood, P. A., Gao, R., Zhang, Y. Q., and Xin, Y. (2020). Mantle influx compensates crustal thinning beneath the Cathaysia Block, South China: evidence from SINOPROBE reflection profiling. *Earth and Planetary Science Letters* 544, 116360. doi:10.1016/j.epsl.2020.116360

Guo, G. A., and Feng, R. (1992). The joint inversion of 3-D velocity structure and source parameters in Xinfengjiang reservoir. *Chinese Journal of Geophysics (in Chinese)* 35 (03), 331–342.

Guo, W., Zhao, C. P., Zuo, K. Z., and Zhao, C. (2022). Characteristics of seismicity before and after impoundment of Baihetan dam in the lower reaches of Jinsha River. *Chinese Journal of Geophysics (in Chinese)* 65 (12), 4659–4671. doi:10.6038/cjg2022Q0119

Han, R., Yang, D., Li, Q., Fu, W., Zhu, G., Zhang, H., et al. (2023). Structural boundary and deep contact relationship between the Yangtze and Cathaysia Blocks from crustal thickness gradients. *Front. Earth Sci* 10, 1065782. doi:10.3389/feart.2022.1065782

Hildebrand, R. S., and Easton, R. M. (1995). An 1161 Ma suture in the Frontenac terrane, Ontario segment of the Grenville orogen. *Geology* 23 (10), 917–920. doi:10.1130/0091-7613(1995)023<0917:amsitf>2.3.co;2

Huang, H. B., Guo, X. W., Xia, S. H., and Qiu, X. L. (2014). Crustal thickness and Poisson's ratio in the coastal areas of South China. *Chinese Journal of Geophysics (in Chinese)* 57 (12), 3896–3906. doi:10.6038/cjg20141204

Huang, H. B., Xiong, H., Qiu, X. L., and Li, Y. (2020). Crustal structure and magmatic evolution in the Pearl River Delta of the Cathaysia Block: new constraints from receiver function modeling. *Tectonophysics* 778, 228365–365. doi:10.1016/j.tecto.2020.228365

Jia, S. X., Li, Z. X., Xu, Z. F., Shen, F. L., Zhao, W. J., Yang, Z. X., et al. (2006). Crustal structure features of the leiqiong depression in hainan province. *Chinese Journal of Geophysics (in Chinese)* 49 (5), 1385–1394. doi:10.1007/BF02006258

Jia, S. X., Zhang, C. K., Zhao, J. R., Fang, S. M., Liu, Z., and Zhao, J. M. (2009). Crustal structure of the rift-depression basin and Yanshan uplift in the northeast part of North China. *Chinese Journal of Geophysics (in Chinese)* 52 (1), 99–110. doi:10.1002/cjg2.1326

Kissling, E., Kradolfer, U., and Maurer, H. (1995). *VELEST user's guide-short introduction, institute of geophysics and Swiss seismological service, user guide*. Zürich: ETH.

Leclère, H., and Calais, É. (2019). A parametric analysis of fault reactivation in the New Madrid Seismic Zone: the role of pore fluid overpressure. *Journal of Geophysical Research Solid Earth* 124 (10), 10630–10648. doi:10.1029/2018JB017181

Li, J. H., Cawood, P. A., Ratschbacher, L., Zhang, Y. Q., Dong, S. W., Xin, Y. J., et al. (2019). Building Southeast China in the late Mesozoic: insights from alternating episodes of shortening and extension along the Lianhuashan fault zone. *Earth-Science Reviews* 201, 103056. doi:10.1016/j.earscirev.2019.103056

Li, J. H., Cawood, P. A., Ratschbacher, L., Zhang, Y. Q., Dong, S. W., Xin, Y. J., et al. (2020). Building Southeast China in the late Mesozoic: insights from alternating episodes of shortening and extension along the Lianhuashan fault zone. *Earth-Science Reviews* 201, 103056. doi:10.1016/j.earscirev.2019.103056

Li, P., Jin, X., Wang, S. X., and Cai, H. T. (2015). Crustal velocity structure of the Shaowu-Nanping-Pingtan transect through Fujian from deep seismic sounding-tectonic implications. *Science China Earth Sciences* 58 (12), 2188–2199. doi:10.1007/s11430-015-5191-6

Li, Q. S., Gao, R., Wu, F. T., Guan, Y., Ye, Z., Liu, Q. M., et al. (2013). Seismic structure in the southeastern China using teleseismic receiver functions. *Tectonophysics* 606, 24–35. doi:10.1016/j.tecto.2013.06.033

Li, S. Y. (2021). *Three dimensional crust mantle velocity structure and deep metallogenic structure in South China*. Beijing: China University of Geosciences.

Lin, J. Y., Xu, T., Cai, H. T., Lv, Q. T., Bai, Z. M., Deng, Y. F., et al. (2021). Crustal velocity structure of Cathaysia Block from an active-source seismic profile between Wanzai and Hui'an in SE China. *Tectonophysics* 811, 228874–874. doi:10.1016/j.tecto.2021.228874

Lin, Y. T., Yu, Y., and Chen, Y. S. (2023). Anisotropic zoning and dynamic mechanism of upper mantle beneath south China block. *Acta Scientiar Naturali Universitatis Pekinensis* 1-8.

Liu, F. T., Xu, P. F., Liu, J. S., Yin, Z. X., Chun, K. Y., Zhang, X. K., et al. (2003). The crustal velocity structure of the continental deep subduction belt: study on the earth Dabie orogen by seismic wide-angle reflection/refraction. *Chinese Journal of Geophysics (in Chinese)* 46 (3), 366–372. doi:10.3321/j.issn:0001-5733.2003.03.014

Liu, T. P., Shao, Y., Yang, X., and Tan, Z. (2017). Determination of the NW-trending faults in Xin-feng-jiang Reservoir dam by using high-precision small earthquake data. *Acta Seismologica Sinica* 39 (1), 23–33. doi:10.11939/jass.2017.01.003

Mackwell, S. J., Zimmerman, M. E., and Kohlstedt, D. L. (1998). High-temperature deformation of dry diabase with application to tectonics on Venus. *Journal of Geophysical Research Solid Earth* 103 (B1), 975–984. doi:10.1029/97JB02671

Majdanski, M. (2013). The uncertainty in layered models from wide-angle seismic data. *Geophysics* 78 (3), WB31–WB36. doi:10.1190/geo2012-0280.1

Majdanski, M., and Polkowski, M. (2014). The uncertainty of 2D models along wide angle seismic profiles. *Pure and Applied Geophysics* 171, 2277–2287. doi:10.1007/s00024-014-0840-9

Mao, J. R., Li, Z. L., and Ye, H. M. (2014). Mesozoic tectono-magmatic activities in South China: retrospect and prospect. *Science China Earth Sciences* 57, 2853–2877. doi:10.1007/s11430-014-5006-1

Moulin, M., Leprêtre, A., Verrier, F., Schnurle, P., Evain, M., Calrens, P. D., et al. (2023). From the Lebombo Monocline to the Mozambique Deep Basin, using combined wide-angle and reflection seismic data. *Tectonophysics* 855, 229814. doi:10.1016/j.tecto.2023.229814

Nazeri, S., Abdi, F., Ismail, A., Rahimi, H., and Zollo, A. (2023). Earthquake source parameters in Zagros region (Iran) from the time-evolutive P-wave displacement. *Scientific Reports* 13 (1), 17964. doi:10.1038/s41598-023-45119-x

Nyamwandha, C. A., Powell, C. A., and Langston, C. A. (2016). A joint local and teleseismic tomography study of the Mississippi Embayment and New Madrid Seismic Zone. *Journal of Geophysical Research Solid Earth* 121 (5), 3570–3585. doi:10.1002/2015JB012761

Qin, J. H., Huang, F., and Wang, D. H. (2022). Batholith recorded mesozoic multistage tectonic evolution of the South China block: a case study of the guandimiao intrusions. *Front. Earth Sci* 10, 948723. doi:10.3389/feart.2022.948723

Qiu, X. L., Wang, Y., Wang, Z. Z., Regenauer-Lieb, K., Zhang, K., and Liu, J. (2018). Determining the origin, circulation path and residence time of geothermal groundwater using multiple isotopic techniques in the Heyuan Fault Zone of Southern China. *Journal of Hydrology* 567, 339–350. doi:10.1016/j.jhydrol.2018.10.010

She, Y. W., Fu, G. Y., Wang, Z. H., and Gao, Y. (2017). Vertical tectonic stress in eastern margin of Bayan Har block revealed by gravity and terrain data. *Chinese Journal of Geophysics (in Chinese)* 60 (6), 2480–2492. doi:10.6038/cjg20170635

Shen, C. G., Chen, H. Q., Zhang, C. H., Huang, L. S., Li, Z. Q., Yang, Z. R., et al. (1974). Xin-feng-jiang reservoir earthquake and its impact on the dam. *Chinese science* (02), 184–205.

Shi, Y. T., and Gao, Y. (2022). Spatial distribution of shear wave splitting of the upper crust in the central South China block. *Chinese Journal of Geophysics (in Chinese)* 65 (9), 3268–3279. doi:10.6038/cjg2022P0741

Shu, L. S., Faure, M., Yu, J. H., and Jahn, B. M. (2011). Geochronological and geochemical features of the Cathaysia block (South China): new evidence for the Neoproterozoic breakup of Rodinia. *Precambrian Research* 187 (3-4), 263–276. doi:10.1016/j.precamres.2011.03.003

Shu, L. S., Wang, B., Cawood, P. A., Santosh, M., Xu, Z. Q., et al. (2015). Early paleozoic and early mesozoic intraplate tectonic and magmatic events in the Cathaysia block, south China. *Tectonics* 34, 1600–1621. doi:10.1002/2015TC003835

Shu, X. J., Jiang, W., Wang, D., Cheng, C., and Wang, H. Z. (2023). Origin and implication of two newly identified peraluminous Atype granites in the early Paleozoic orogeny, Southeast Asia. *Front. Earth Sci* 11, 1137157. doi:10.3389/feart.2023.1137157

Sibson, R. H. (1983). Continental fault structure and the shallow earthquake source. *Geolo. Soc. Lond* 140, 741–767. doi:10.1144/gsjgs.140.5.0741

Song, X. H., Pan, S. Z., Wang, F. Y., Tian, X. F., Liu, B. F., and Song, J. J. (2024). Deep crustal structure and deformation features of the northeastern margin of the Tibetan Plateau, as revealed by controlled-source seismic profiling along the Aba-Guyuan-Wuqi transect. *Tectonophysics* 885, 230418. doi:10.1016/j.tecto.2024.230418

Tannock, L., and Regenauer-Lieb, K. (2017). The Heyuan Fault, south China: a deep geothermal prospect – the role of fault intersection relationships and fluid flow. *39th N. Z. Geothermal Workshop 22 - 24 November*, 2017. doi:10.1190/GEM2015-049

Tannock, L., Wang, Y., Liu, J., Li, J. F., Zhang, K., Xu, L. F., et al. (2019). A preliminary investigation on the geothermal genesis of the Guangdong Heyuan Fracture Zone and its relationship with tectonics. *Journal of Geomechanics* 25 (03), 400–411. doi:10.12090/j.issn.1006-6616.2019.25.03.037

Tannock, L. H., Berger, M., Liu, J., and Regenauer-Lieb, K. (2020). The effects of a tectonic stress regime change on crustal-scale fluid flow at the Heyuan geothermal fault system. South China. *Tectonophysics* 781, 228–399. doi:10.1016/j.tecto.2020.228399

Tarayoun, A., Mazzotti, S., and Gueydan, F. (2019). Quantitative impact of structural inheritance on present-day deformation and seismicity concentration in intraplate deformation zones. *Earth Planet. Sci. Lett* 518, 160–171. doi:10.1016/j.epsl.2019.04.043

Tian, X. F., Xiong, W., Wang, F. Y., Xu, C. F., Duan, Y. H., and Jia, S. X. (2020). Upper crustal velocity structure and constraining fault interpretation from Shunyi-Tanggu refraction experiment data. *Seismogeology* 42 (02), 414–434. doi:10.3969/j.issn.0253-4967.2020.02.011

Tiira, T., Janik, T., Veikkolainen, T., Komminaho, K., Skrzynik, T., Vakeva, S., et al. (2022). Implications on crustal structure from the South Finland Coastal (SOFIC) deep seismic sounding profile. *Bulletin of the Geological Society of Finland* 94 (2), 165–180. doi:10.17741/bgsf/94.2.004

Vidale, J. E. (1990). Finite-difference calculation of travel times in three dimensions. *Geophysics* 55, 521–526. doi:10.1190/1.1442863

Wan, Y. K., Liu, X., Liu, R. F., Zhang, Y., Shen, X. Q., and Zheng, Z. J. (2022). Numerical simulation of the present deformation pattern in the crust and top of the upper Mantle in the Songpan-Garzê block. *Chinese Journal of Geophysics (in Chinese)* 65 (7), 2484–2502. doi:10.6038/cjg2022P0235

Wang, G. Z., Chen, Y. S., Zhang, C., Ge, Z. X., Guo, Z., Yang, T., et al. (2022). Mantle transition zone thickness anomaly at middle Southern China by receiver function: evidence for Hainan Plume. *Chinese Journal of Geophysics (in Chinese)* 65 (10), 3871–3880. doi:10.6038/cjg2022P0338

Wang, S. (2020). *Ambient noise surface wave tomography using a dense array and its applications*. Guangzhou institute of geochemistry, Chinese Academy of Sciences. doi:10.27544/d.cnki.gzcds.2020.000006

Wang, S. J., Liu, B. J., Zhang, J. S., Liu, B. F., Duan, Y. H., Song, X. H., et al. (2015a). Study on the velocity structure of the crust in Southwest Yunnan of the north-south seismic belt-Results from the Menghai-Gengma-Lushui deep seismic sounding profile. *Science China EarthSciences* 58, 2175–2187. doi:10.1007/s11430-015-5189-0

Wang, S. J., Wang, F. Y., Zhang, J. S., Liu, B. F., Zhang, C. K., and Zhao, J. R. (2015b). The deep seismogenic environment of Lushan MS7.0 earthquake zone revealed by a wide-angle reflection/refraction seismic profile. *Chinese Journal of Geophysics (in Chinese)* 58 (9), 3193–3204. doi:10.6038/cjg20150915

Westgate, M., Manzi, M. S. D., James, I., Andreoli, M. A. G., and Durrhein, R. (2022). Seismic constraints on the trompsburg layered igneous intrusion complex in South Africa using two deep reflection seismic profiles. *Front. Earth Sci* 10, 839995. doi:10.3389/feart.2022.839995

Willis, K., Houseman, G. A., Evans, I., Wright, T., and Hooper, A. (2019). Strain localization by shear heating and the development of lithospheric shear zones. *Tectonophysics* 764, 62–76. doi:10.1016/j.tecto.2019.05.010

Xi, J. J. (2021). *Study on the velocity structure of crust and mantle in the deep of the Nanling Mountain tectonic belt and Cathaysia block*. Beijing: China University of Geosciences.

Xia, S. R., Shi, L., Li, Y. H., and Guo, L. H. (2021). Tibetan plateau revealed by double-difference tomography. *Chinese Journal of Geophysics (in Chinese)* 64 (9), 3194–3206. doi:10.6038/cjg2021O0514

Xie, G. Q., Hu, R. Z., Zhao, J. H., and Jiang, G. H. (2001). Mantle plume and the relationship between it and mesozoic large-scale ore Formation in Southeastern China. *Geotectonics and Metallogeny* 02, 179–186.

Xiong, X. S., Wang, G., Li, Q. S., Lu, Z. W., Gao, R., Feng, S. Y., et al. (2022). Crustal structure of the chuan-dian block revealed by deep seismic sounding and its implications for the outward expansion of the East Tibetan plateau. *Acta Geologica Sinica-English Edition* 96 (6), 1932–1944. doi:10.1111/1755-6724.14922

Xu, X. B., Zhang, Y. Q., Jia, D., Shu, L. S., and Wang, R. R. (2009). Early mesozoic geotectonic processes in south China. *Geology of China* 36 (03), 573–593. doi:10.1016/S1874-8651(10)60080-4

Xu, X. W., Wu, X. Y., Yu, G. H., Tan, X. B., and Li, K. (2017). Seismo-geological signatures for identifing Ms ≥7.0 earthquake risk areas and their premilimary application in mainland China. *Earthquake Geology* 39 (2), 219–275. doi:10.3969/j.issn.0253-4967.2017.02.001

Yan, X., Xu, X. S., Zhao, G. C., and Liu, L. (2015). Neoproterozoic active continental margin of the Cathaysia block: evidence from geochronology, geochemistry, and Nd–Hf isotopes of igneous complexes. *Precambrian Research* 269, 195–216. doi:10.1016/j.precamres.2015.08.006

Yang, X., Li, Y., Afonso, J. C., Yang, Y., and Zhang, A. (2021). Thermochemical state of the upper mantle beneath South China from multi-observable probabilistic inversion. *Journal of Geophysical Research Solid Earth* 126, e2020JB021114. doi:10.1029/2020JB021114

Yang, X. S., Ma, J., and Zhang, X. J. (2003). A review of the genesis of the low speed layer in the continental crust. *Geological Science and Technology Information* 02, 35–41. doi:10.3969/j.issn.1000-7849.2003.02.008

Yang, Z. X., Liu, B. F., Wang, Q. C., and Wang, H. T. (2011). 2-D p-wave velocity structure in the Xin-feng-jiang reservoir area-Results of Yingde-Heyuan-Luhe deep seismic sounding profile. *Progress in geophysics* 26 (06), 1968–1975. doi:10.3969/j.issn.1004-2903.2011.06.010

Yang, Z. X., Liu, B. F., Wang, Q. C., Zhao, C. P., Chen, Z. L., and Zhang, X. K. (2013). Tomographic imaging of the upper crustal structure beneath the Xinfengjiang reservoir area. *Chinese Journal of Geophysics (in Chinese)* 56 (4), 1177–1189. doi:10.6038/cjg20130413

Ye, X. W., Deng, Z. H., Huang, Y. M., Liu, J. P., Wang, X. N., Liu, J., et al. (2017). The characteristics of 3D P-wave velocity structure of Middle-uppper crust and reservoir water infiltration-diffusion in Xin-feng-jiang Reservoir of Guangdong. *Chinese Journal of Geophysics (in Chinese)* 60 (09), 3432–3444. doi:10.ssss/j.issn.0001-5733.2017.9.012

Ye, X. W., Lv, Z. Y., Wang, L., Song, J. J., Duan, Y. H., Wang, S. J., et al. (2024). Fine crustal velocity structure revealed by a deep seismic sounding profile of Lianping-Heyuan-Shanwei in the Eastern Guangdong. *Chinese Journal of Geophysics (in Chinese)* 67 (6), 2304–2321. doi:10.6038/cjg2022Q0737

Ye, X. W., Zhang, X., Lv, J. S., Liu, B. F., Wang, X. N., Wang, L. W., et al. (2020). Crustal structure and tectonic attribute revealed by a deep seismic sounding profile of Dinghu-Gaoming-Jinwan in the Pearl River delta. *Chinese Journal of Geophysics (in Chinese)* 63 (5), 1959–1969. doi:10.6038/cjg2020M0378

Yue, H., Zhang, Z. Q., and Chen, Y. J. (2008). Interaction between adjacent left-slip and retrograde faults: the 1976 Songpan earthquake complex. *Scientific Bulletin* 53 (13), 1582–1588. doi:10.1007/s11434-008-0210-z

Zelt, C. A., and Smith, R. B. (1992). Seismic traveltime inversion for 2-D crustal velocity structure. *Geophys J Int* 108, 16–34. doi:10.1111/j.1365-246x.1992.tb00836.x

Zeng, R. S., Lu, H. H., and Ding, Z. F. (1988). Discussion on the genesis of the tangshan earthquake from the results of seismic refraction and reflection sections. *Chinese Journal of Geophysics (in Chinese)* 31 (04), 383–398.

Zeng, R. S., Zhang, S. Q., Zhou, H. N., and He, Z. N. (1985). Crustal structure of Tangshan epicentral region and its relation to the seismogenic process of a continental earthquake. *Seismology and Geology* 02, 125–142.

Zhan, Y., Hou, G. T., Kusky, T., and Gregg, P. M. (2016). Stress development in heterogenetic lithosphere: insights into earthquake processes in the New Madrid Seismic Zone. *Tectonophysics* 671, 56–62. doi:10.1016/j.tecto.2016.01.016

Zhang, G. Q., Zhu, Y. Q., and Liang, W. F. (2022). The crustal density structure and isostatic additional stress around the Fubianhe fault on the eastern margin of Tibet plateau. *Seismology and geology* 44 (3), 578–589. doi:10.3969/j.issn.0253-4967.2022.03.002

Zhang, G. W., Guo, A. L., Wang, Y. J., Li, S. Z., Dong, Y. P., Liu, S. P., et al. (2013). Tectonics of South China continent and its implications. *Science China Earth Sciences* 56, 1804–1828. doi:10.1007/s11430-013-4679-1

Zhang, H., Cheng, H. D., Pang, Y. J., Shi, Y., and Yuen, D. A. (2016). Influence of the impoundment of the three gorges reservoir on the micro-seismicity and the 2013 M5.1 badong earthquake (Yangtze, China). *Physics of the Earth and Planetary Interiors* 261 (A), 98–106. doi:10.1016/j.pepi.2016.06.007

Zhang, X. K., Yang, Y. C., Zhao, P., Zhao, J. R., Luo, L. L., Wang, C. L., et al. (1994). Three-dimensional seismic transmission study of the Tangshan-Luanxian seismic zone-velocity tomography of the middle and upper crust. *Geophysical Journal* 06, 759–848.

Zhao, J. L., Qiu, J. S., Liu, L., and Wang, R. Q. (2016). The Late Cretaceous I- and A-type granite association of southeast China: implications for the origin and evolution of post-collisional extensional magmatism. *Lithos* 240, 16–33. doi:10.1016/j.lithos.2015.10.018

Zhou, P. X., Xia, S. H., Hetényi, G., Monteiller, V., and Sun, J. (2020). Seismic imaging of a mid-crustal low-velocity layer beneath the northern coast of the South China Sea and its tectonic implications. *Physics of the Earth and Planetary Interiors* 308, 106573. doi:10.1016/j.pepi.2020.106573

Zhu, J. Z., and Sun, Y. J. (2022). Numerical simulation of the effect of water storage on seismic activity in Dagangshan Reservoir, Sichuan, China. *Chinese Journal of Geophysics (in Chinese)* 65 (10), 3930–3943. doi:10.6038/cjg2022P0742

Zuza, A. V., Cao, W., Rodriguez-Arriaga, A., Desormeau, J. W., and Odlum, M. L. (2022). Strain localization at brittle-ductile transition depths during Miocene magmatism and exhumation in the southern Basin and Range. *Journal of Structural Geology* 163, 104709. doi:10.1016/j.jsg.2022.104709